

L.J.M. Houben, A.A.A. Molenaar, G.H.A.M. Fuchs, H.O. Moll

Laboratory for Road and Railroad Research, Delft University of Technology, Delft, The Netherlands

ABSTRACT

A design (and evaluation) method for concrete block pavements, consisting of 80 mm thick rectangular concrete blocks in herringbone bond and a sand subbase, is described. The method is based on the results of falling weight deflection measurements that were carried out in 1982 on 17 in service concrete block pavements in the city of Delft. From these measurements it appeared that all deflections as well as the surface curvature index SCI decreased with increasing number of equivalent 80 kN standard axle loads as applied on the surveyed sections. The deflection measurements were analyzed by means of the linear-elastic multilayer program CIRCLY and by means of the finite element program ICES STRUDL in which the concrete blocks were represented as indeformable rigid bodies. With the ICES STRUDL program an excellent correspondence between measured and calculated deflection curves was obtained. The deflection curves calculated by means of the CIRCLY program were different from the measured deflection curves, especially if the pavement section was subjected to a limited number of load repetitions. From the analysis of the measurements it appeared that the stiffness of the substructure (sand subbase plus subgrade), the bedding layer and the joints between the concrete blocks all increased with increasing number of load repetitions. Functions have been developed to describe this progressive stiffening in time. Based on the result of the analysis charts have been developed for the design of concrete block pavements, consisting of 80 mm thick rectangular concrete blocks in herringbone bond and a sand subbase. These charts enable to determine the pavement life as a function of the initial substructure modulus, the thickness of the sand subbase, the number of equivalent 80 kN standard axle loads per lane per day and the acceptable rut depth. Furthermore it was determined that the stiffness of the bedding layer and the joints increased with decreasing surface curvature index SCI; the relations also cover concrete block pavements that have a bound or unbound base. It also appeared that both the bedding layer and the joint stiffness are dependent on the magnitude of the equivalent elastic modulus of the substructure (base plus sand subbase plus subgrade); a maximum value for both parameters is reached at an equivalent substructure modulus of 550 N/mm².

1. INTRODUCTION

This paper describes the development of a design method for concrete block pavements with a sand subbase only, a pavement structure that is widely used in The Netherlands for normal road traffic. Until now there has been done hardly any research on this pavement structure (1), so there is rather a lack of knowledge concerning the actual in service behaviour. This knowledge is necessary in order to be able to develop more rational design and maintenance strategies. In order to improve the readability of the paper, a summary of the various chapters will be given here.

Chapter 2 describes the analysis of a number of concrete block pavements in the city of Delft by means of the linear-elastic multilayer theory. The pavements consist of 80 mm thick rectangular concrete blocks in herringbone bond and a sand subbase with varying thickness. The input for the analysis was obtained from falling weight deflection measurements.

In chapter 3 some characteristic Delft pavements as well as some concrete block pavements with a bound or unbound base are analyzed by means of a finite element model. In this model the concrete blocks are represented as indeformable rigid bodies.

In chapter 4 for the Delft pavements a comparison is made between the results of the analyses as performed by means of the linear-elastic multilayer theory and the finite element model. In chapter 5 a method for the calculation of the permanent deformation in granular and cohesive materials is presented. This method is used to calculate the rutting development of the Delft pavements.

Finally design charts for concrete block pavements, consisting of 80 mm thick rectangular concrete blocks in herringbone bond and a sand subbase, are presented in chapter 6. These design charts are based on a number of rut depth calculations.

It should be noted that the presented design method for concrete block pavements is only applicable if shear failure in the sand subbase is not likely to occur. From the observations it was concluded that this is the case if the surface curvature index SCI as measured by means of a falling weight (F = 50 kN) is less than 1300 μm (2,3).

2. ANALYSIS OF CONCRETE BLOCK PAVEMENTS IN DELFT BY MEANS OF THE LINEAR-ELASTIC MULTILAYER THEORY

In 1982 falling weight deflection measurements

have been carried out on 17 in service concrete block pavements in the city of Delft (4). In such a deflection measurement a 50 kN dynamic load is applied on the pavement by means of a circular plate diameter 300 mm, so the contact pressure equals $0,707 \text{ N/mm}^2$; the loading time is 0,02 s. The deflections (d) have been measured in the inner wheeltrack (T) and in the middle between the wheeltracks (M) at distances of 0, 300, 500, 1000, 1500 and 2000 mm from the centre of the loading plate.

2.1 Pavement characteristics

Some characteristics of the concrete block pavements in Delft are:

- rectangular concrete blocks, dimensions $l \times w \times h = 210 \times 105 \times 80 \text{ mm}$, in herringbone bond
- sand subbase, thickness 0,85 to 1,4 m and more (table 1)
- clay subgrade (Dutch cone penetrometer value 0,5 to 1 $\text{N/mm}^2 \cong \text{CBR-value } 2 \text{ to } 4\%$).

For the linear-elastic multilayer calculations this pavement structure was schematized into a twolayer system, where the toplayer (elastic modulus E_1 , Poisson's ratio ν_1) represents the concrete block layer and the second layer

(elastic modulus E_0 , Poisson's ratio ν_0) represents the substructure, consisting of the sand subbase and the subgrade (figure 1).

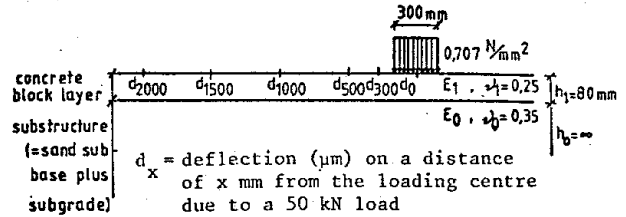


Figure 1. Schematization of the Delft concrete block pavements for the linear-elastic multilayer calculations.

2.2 Traffic loading

For the analyzed pavements best possible estimates of the cumulative historical traffic loading n (the number of equivalent 80 kN standard axle loads) were made on basis of mechanical and visual traffic countings, public bus time schedules and bus axle loads (table 1). The applied load equivalency factor l_e is: $l_e = (L/80)^4$, where L = axle load (kN).

pavement no.	thickness sand subbase h_{sa} (m)	traffic loading		location deflection measurement	deflections (μm)						SCI (μm)
		n	$\log n$		d_0	d_{300}	d_{500}	d_{1000}	d_{1500}	d_{2000}	
1	> 1,40	942.100	5,97	T	661	337	193	103	68	51	468
				M	701	382	213	99	63	45	488
2	1,20	113.145	5,05	T	653	365	178	101	71	52	475
				M	709	361	191	115	81	59	518
5	1,03	1.130.020	6,05	T	722	403	229	110	71	49	493
				M	623	339	181	81	58	43	442
6	0,85	68.770	4,84	T	646	363	202	110	73	54	444
				M	642	327	194	89	68	52	448
7	1,00	25.790	4,41	T	1387	602	342	177	127	96	1045
				M	1243	599	340	203	123	98	903
8	> 1,40	25.790	4,41	T	942	363	228	139	112	77	714
				M	1080	485	251	150	123	90	829
9	1,15	17.190	4,24	T	1404	712	403	185	140	103	1001
				M	1433	666	395	207	146	114	1038
10A	1,03	858.660	5,93	T	913	442	238	137	92	69	675
				M	826	420	237	122	85	67	589
10B	1,03	792.760	5,90	T	910	391	221	123	81	63	689
				M	927	407	240	119	86	67	687
11	0,90	66.830	4,82	T	1413	788	580	312	214	152	833
				M	1542	854	553	322	229	151	989
12	> 1,40	66.830	4,82	T	946	464	231	131	95	73	715
				M	758	390	213	118	89	66	545
13	1,10	386.820	5,59	T	613	346	213	122	88	65	400
				M	842	386	239	136	91	65	603
14	1,13	297.170	5,47	T	673	326	178	101	71	51	495
				M	767	368	199	105	69	50	568
15	1,24	146.120	5,16	T	701	335	198	124	90	66	503
				M	802	323	196	123	91	65	606
16	1,00	66.830	4,82	T	893	448	280	180	130	100	613
				M	1071	516	310	207	146	107	761
17	> 1,40	66.830	4,82	T	913	399	234	152	112	79	679
				M	900	391	227	146	108	81	673
19	1,33	1.000	3,00	T	876	479	282	175	118	82	594
				M	853	461	270	156	117	87	583

Table 1. Review of the sand subbase thickness, the traffic loading and the mean measured deflection curves of the Delft pavements.

2.3 Test results

For each of the 17 pavements the mean deflection curve as well as the surface curvature index SCI ($= d_0 - d_{500}$) are given in table 1, both for the inner wheeltrack (T) and for the middle between the wheeltracks (M).

2.4 Processing and interpretation of the deflection data

For the statistical processing of the deflection data the analyzed pavements are divided into 4 classes of sand subbase thickness (table 2). Considering the number of pavements per class, statistical relations will only be determined for classes C and E.

By means of linear regression analysis relations between the various deflections d_x respectively the surface curvature index SCI on one hand and the traffic loading n on the other hand were determined.

The relation between the maximum deflection d_0 (μm) and the traffic loading n is (figure 2):

$$\begin{aligned} \text{class C, T: } d_0 &= 2726 - 337 \log n & r &= -0,79 & (1a) \\ \text{M: } d_0 &= 2790 - 344 \log n & r &= -0,92 & (1b) \\ \text{class E, T: } d_0 &= 1851 - 197 \log n & r &= -0,96 & (1c) \\ \text{M: } d_0 &= 1869 - 202 \log n & r &= -0,80 & (1d) \end{aligned}$$

For the relation between the surface curvature index SCI (μm) and the traffic loading n was found (figure 3):

$$\begin{aligned} \text{class C, T: } \text{SCI} &= 1985 - 247 \log n & r &= -0,75 & (2a) \\ \text{M: } \text{SCI} &= 2017 - 249 \log n & r &= -0,91 & (2b) \\ \text{class E, T: } \text{SCI} &= 1498 - 171 \log n & r &= -0,97 & (2c) \\ \text{M: } \text{SCI} &= 1549 - 183 \log n & r &= -0,81 & (2d) \end{aligned}$$

Both in class C and class E all deflections as well as the surface curvature index decrease with increasing traffic loading n . At a limited number of load repetitions (e.g. $n = 1000 \hat{=} \log n = 3$) a larger sand subbase thickness gives smaller deflections, but after many load repetitions ($n = 1000000 \hat{=} \log n = 6$) the deflections are nearly independent of the sand subbase thickness; for the pavement structure considered the load spreading reaches an optimum value after $n = 1000000$.

In general the deflections in the inner wheel-track (T) are something less than the deflections in the indirectly loaded area between the wheeltracks (M).

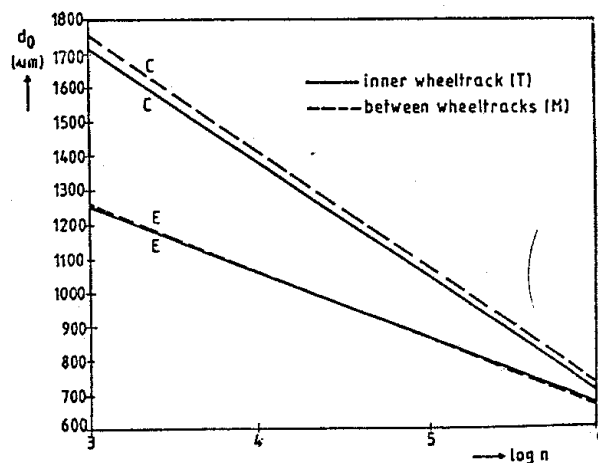


Figure 2. Relationship between the maximum deflection d_0 and the traffic loading n for the Delft pavements.

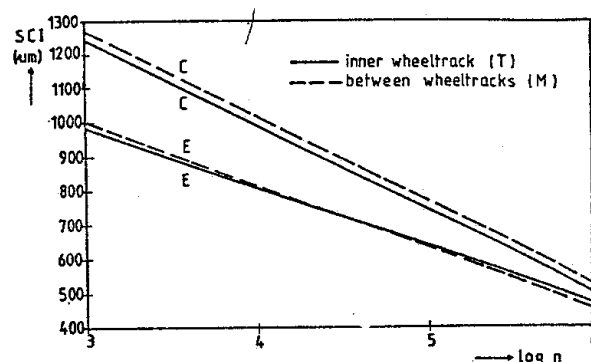


Figure 3. Relationship between the surface curvature index SCI and the traffic loading n for the Delft pavements.

The elastic modulus of the substructure E_0 (N/mm^2) was calculated from the deflection (μm) measured at a distance of 2000 mm from the centre of the loading plate (d_{2000}) by means of the formula (5):

$$\log E_0 = 3,869 - 1,009 \log d_{2000} \quad (3)$$

For the determination of the elastic modulus of the concrete block layer (E_1) linear-elastic multilayer calculations with the computer program CIRCLY (6) were carried out for various combinations of E_1 and E_0 in the twolayer system, shown in figure 1 (4). From the results of these calculations a graph was developed, giving (for a concrete block thickness of 80 mm) the elastic modulus E_1 as a function of the maximum deflection d_0 .

class	thickness sand subbase h_{sa} (m)	traffic loading n						
		< 10.000	10.000	50.000	100.000	250.000	500.000	> 1.000.000
B	0,80 - 1,00							
C	1,00 - 1,20							
D	1,20 - 1,40	19	7, 9	6, 11	2, 15	13, 14	10A, 10B	5
E	> 1,40		8	12, 17			1	

Table 2. Division of the Delft pavements into 4 classes of sand subbase thickness.

and the surface curvature index SCI (figure 4). By means of figure 4 also the elastic modulus of the substructure E_0 can be determined. However, in this way a E_0 -value is found that differs from equation 3. This illustrates that concrete block pavements, especially in their early life, do not behave like linear-elastic multilayer systems. We will come back on this subject in chapter 4.

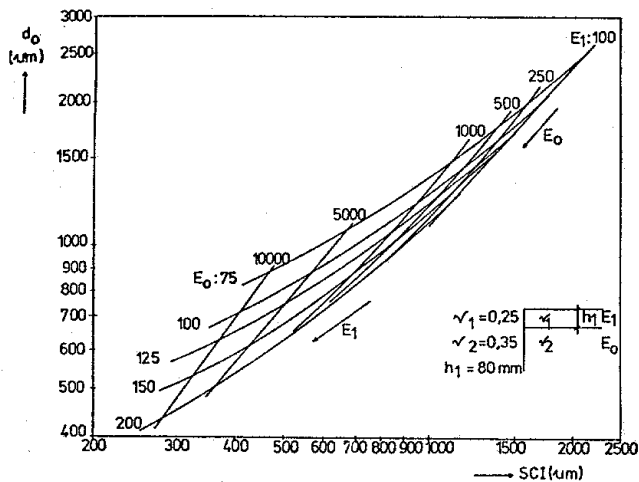


Figure 4. Graph for the determination of the elastic moduli in a two-layer system with $h_1 = 80$ mm.

From the deflections measured on the various Delft pavements (table 1) the elastic moduli E_0 and E_1 of the substructure respectively the concrete block layer were calculated by means of equation 3 respectively figure 4.

By means of linear regression analysis relations between the elastic moduli E_0 respectively E_1 and the traffic loading n were determined. For the relation between the elastic modulus of the substructure E_0 (N/mm^2) and the traffic loading n was found (figure 5):

class C, T:	$E_0 = -94,6 + 38,8 \log n$	$r = 0,87$	(4a)
M:	$E_0 = -131,2 + 46,0 \log n$	$r = 0,82$	(4b)
class E, T:	$E_0 = -37,3 + 30,1 \log n$	$r = 0,89$	(4c)
M:	$E_0 = -150,3 + 52,4 \log n$	$r = 0,98$	(4d)

The relation between the elastic modulus of the concrete block layer E_1 (N/mm^2) and the traffic loading n is (figure 6):

class C, T:	$E_1 = -3529 + 1243 \log n$	$r = 0,47$	(5a)
M:	$E_1 = -2427 + 988 \log n$	$r = 0,68$	(5b)
class E, T:	$E_1 = -1719 + 918 \log n$	$r = 0,72$	(5c)
M:	$E_1 = -3235 + 1221 \log n$	$r = 0,80$	(5d)

From the equations 4 and 5 and the figures 5 and 6 it can be seen that the elastic moduli increase with increasing number of load repetitions. So the structural behaviour of concrete block pavements improves in time, in contrast to flexible and rigid pavements.

At a limited number of load repetitions (e.g. $n = 1000 \approx \log n = 3$) a larger sand subbase thickness yields a better structural behaviour, but after many load repetitions ($n = 1000000 \approx \log n = 6$) the structural behaviour is nearly independent

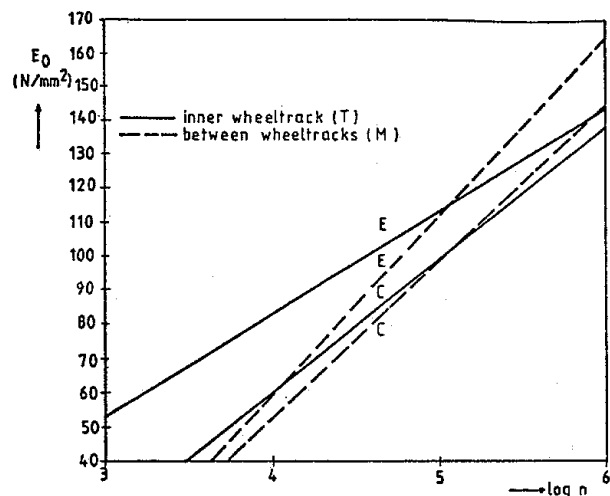


Figure 5. Relationship between the elastic modulus of the substructure E_0 and the traffic loading n for the Delft pavements.

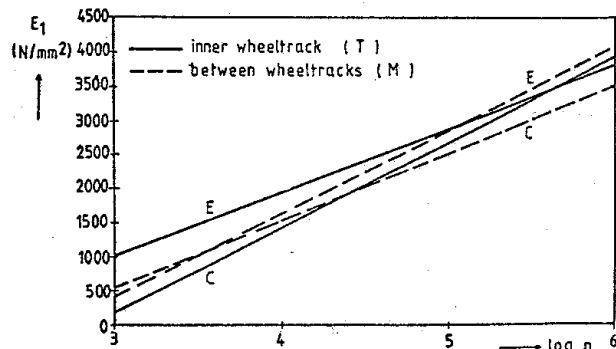


Figure 6. Relationship between the elastic modulus of the concrete block layer E_1 and the traffic loading n for the Delft pavements.

of the sand subbase thickness: the load spreading has reached an optimum value. In general the structural behaviour in the wheel-track (T) is a little bit better than in the indirectly loaded area between the wheeltracks (M).

With regard to the interaction between the concrete block layer and the substructure the following relations between E_1 and E_0 (N/mm^2) were found (figure 7):

class C, T:	$E_1 = 25 E_0 + 296$	$r = 0,43$	(6a)
M:	$E_1 = 21 E_0 + 490$	$r = 0,80$	(6b)
class E, T:	$E_1 = 36 E_0 - 1173$	$r = 0,95$	(6c)
M:	$E_1 = 26 E_0 - 10$	$r = 0,90$	(6d)

From equation 6 and figure 7 it can be seen that for the Delft pavements the load spreading in the concrete block layer increases with increasing stiffness (support) of the substructure. This subject is further dealt with in chapter 3.

3. ANALYSIS OF CONCRETE BLOCK PAVEMENTS BY MEANS OF THE FINITE ELEMENT METHOD

Some of the Delft pavements and a number of other

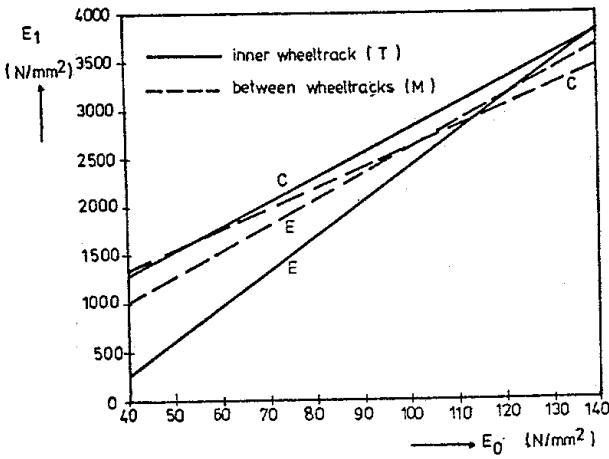


Figure 7. Relationship between the elastic moduli of the concrete block layer E_1 and the substructure E_0 for the Delft pavements.

concrete block pavements have been analyzed by means of a finite element program. In this case the ICES STRUDL program was selected since recently a special element type, called RIGID BODY, has come available that could be used for a proper schematisation of the concrete blocks (7).

3.1 Characteristics of the analyzed pavements

- By means of ICES STRUDL calculations the following concrete block pavements were analyzed (8):
- ECT container terminal in Rotterdam (9); the pavement consists of 120 mm thick rectangular concrete blocks, 50 mm gravel 0/8 mm, 330 mm sandcement base and 1 to 2 m sand subbase on a clay subgrade
 - Truck Centre (TC) in Rotterdam; the pavement consists of 90 mm thick rectangular concrete blocks, 50 mm bedding sand, 300 mm unbound base and 1 to 2 m sand subbase on a clay subgrade
 - some characteristic Delft pavements (4): no. 2, 7, 10 and 19 (table 1)
 - two prototype pavements (PP), consisting of 80 respectively 120 mm thick rectangular concrete blocks on a sand subgrade (2,3); the pavements were subjected to repeated plate loadings.

3.2 Modelling of the concrete block pavements

In principle the design problem is three-dimensional (figure 8a). However, because of axisymmetry the three-dimensional problem reduces to a two-dimensional case, similar to a plane strain problem (figure 8b); tangential displacements (i.e. in the circumferential direction) do not exist, and stresses and strains do not vary in the circumferential direction. For reasons of symmetry the model of figure 8b is reduced further to the model of figure 8c (8). The thickness of the model is set at 1 mm. The indeformable basis is taken at a depth of 5,56 m; initial CIRCLY calculations made clear that at this depth the stresses due to a falling weight loading are neglectable. Because the vertical forces and horizontal displacements are neglectable at the edge of the model, that is 3,2 m from the loading centre, the right hand side

edge is laid on rollers incapable of transmitting vertical forces. The deflection measurements on the various concrete block pavements indicated that the shape of the deflection bowl was very much alike the deflection curve of a pure shear layer pavement; assuming the concrete block layer behaves like a pure shear layer implicates that no horizontal forces are transmitted in the joints and that no rotation of the blocks occurs.

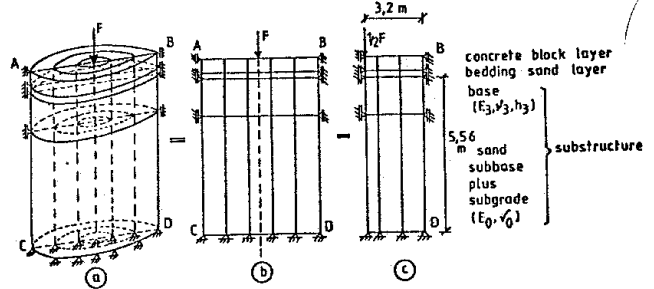


Figure 8. Modelling of concrete block pavements for calculations with the finite element program ICES STRUDL.

The concrete block layer is schematized by a number of rigid bodies, that represent the concrete blocks, joined together by means of vertical linear springs, that represent the shear resistance of the joints. The spring stiffness k (N/mm) of the joints is:

$$k = \frac{G \cdot h_1 \cdot l}{2 \cdot v} = \frac{G \cdot h_1}{2 \cdot v} \quad (7)$$

where: G = shear modulus of the joints (N/mm²)
 h_1 = concrete block thickness (mm)
 v = joint width (mm)

The bedding sand layer is represented by vertical linear springs. The spring stiffness k' (N/mm) is:

$$k' = \frac{c \cdot b \cdot l}{2} = \frac{c \cdot b}{2} \quad (8)$$

where: c = bedding constant (N/mm³)
 b = concrete block length or width (mm), considering herringbone bond

Figure 9 shows the modelling of the concrete block layer and the bedding sand layer.

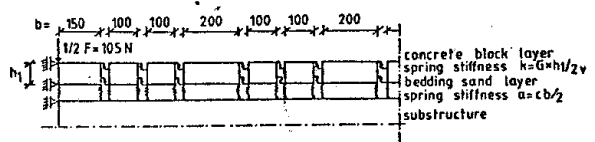


Figure 9. Modelling of concrete block layer and bedding sand layer for ICES STRUDL calculations.

The layers beneath the bedding sand layer are supposed to be homogeneous, isotropic and linear-elastic. They are characterized by their elastic modulus E and Poisson's ratio ν .

The elastic modulus of the sand subbase plus the subgrade E_0 is calculated by means of equation 3. Poisson's ratio ν_0 is set at 0,35.

In order to be able to analyse from the deflection curve the structural properties of the concrete block layer of a multilayered pavement with a bound base, like the one applied at the ECT container terminal, the elastic modulus of the base need to be known. Therefore a method to assess the base modulus was derived from extensive CIRCLY calculations and by using Odemark's equivalency theory (9). The elastic modulus of the sandcement base E_3 (N/mm^2) is calculated from:

$$E_3 = 100. \left(\frac{h_e - h_e^x}{0,33} \right)^3 \quad (9)$$

$$\text{where: } h_e = 1,919 - 2,458. \log \left(\frac{d_{500} - d_{1500}}{50} \right) \quad (10)$$

$$h_e^x = 0,4876 - 0,3747. \log \left(\frac{d_0 - d_{200}}{50} \right) \quad (11)$$

h_e = equivalent layer thickness (m) of concrete block layer plus bedding sand layer plus bound base

$$(h_e = h_1 \sqrt[3]{\frac{E_1}{E_0}} + h_2 \sqrt[3]{\frac{E_2}{E_0}} + h_3 \sqrt[3]{\frac{E_3}{E_0}})$$

h_e^x = equivalent layer thickness (m) of concrete block layer plus bedding sand layer

$$(h_e^x = h_1 \sqrt[3]{\frac{E_1}{E_0}} + h_2 \sqrt[3]{\frac{E_2}{E_0}})$$

d_x = deflection (μm) on a distance of x mm from the loading centre

Poisson's ratio ν_3 of the sandcement base is set at 0,2.

The elastic modulus E_3 (N/mm^2) of the unbound base of the Truck Centre (TC) pavement is calculated by means of the following empirical equation (10):

$$E_3 = 1.E_0 \quad \text{with } l = 0,206.h_3^{0,45} \quad (2 \leq l \leq 4) \quad (12)$$

where: h_3 = thickness unbound base (mm)

Poisson's ratio ν_3 of the unbound base is set at 0,35.

3.3 Results of the calculations

By means of the finite element representation an excellent correspondence between the calculated and measured deflection curves was obtained (8). In figure 10 this is illustrated for one of the Delft pavements and for one deflection measurement on the ECT container terminal.

The measured deflections as well as the calculated elastic moduli of the sand subbase plus the subgrade (E_0) and the base (E_3) of the various analyzed pavements are summarized in table 3. Furthermore the values of the bedding constant c and the joint stiffness k , calculated with ICES STRUDEL by means of trial and error, are given. The pavements of ECT (sandcement base) and Truck Centre (unbound base) as well as the Delft pave-

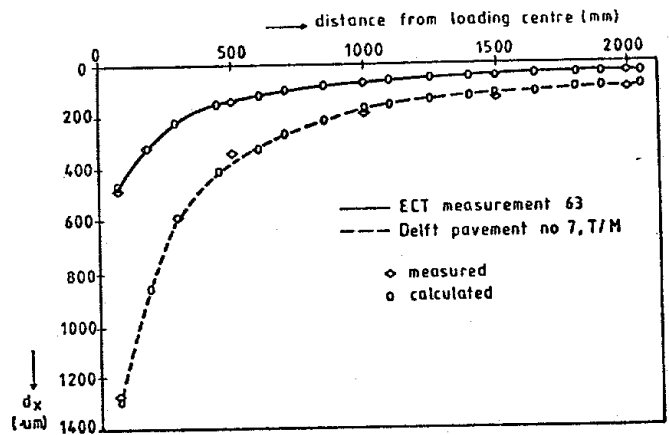


Figure 10. Two examples of measured and ICES STRUDEL calculated deflection curves.

ments (without a base) had been subjected to vehicular traffic, however the prototype pavements (without a base) were subjected to repeated plate loadings. Comparison of the various c - and k -values leads to the conclusion that c and k are dependent of both the substructure of the pavement and the traffic loading (see further sections 3.4 and 3.5).

On basis of the calculated c - and k -values general relations between the bedding constant c (N/mm^3) respectively the joint stiffness k (N/mm) and the surface curvature index SCI (μm) have been derived (8) (the various k -values are comparable because, as is known from construction practice, the quotient h_1/v in equation 7 is nearly constant). These relations are (figures 11 and 12):

$$c = \frac{SCI}{(38,08488 + 0,147263.(SCI - 200))^2} \quad (13)$$

$$k = \frac{SCI}{(1,932189 + 0,005022.(SCI - 200))^3} \quad (14)$$

The relation between k and c is:

$$k = (45)^3 \cdot \frac{d(c)}{d(SCI)} \quad (15)$$

3.4 Relationship between the bedding constant c respectively the joint stiffness k and the equivalent elastic modulus of the substructure E_{eq}

For the pavements mentioned in table 3 the equivalent elastic modulus of the substructure E_{eq} was calculated from the elastic modulus (E_3) $_{eq}$ and the thickness (h_3) of the base and the elastic modulus of the sand subbase plus subgrade (E_0) using Ivanov's equivalency theory (11). For the pavements without a base holds: $E_{eq} = E_0$. The general relations between the bedding constant c (N/mm^3) respectively the joint stiffness k (N/mm) and the equivalent elastic modulus of the substructure E_{eq} (N/mm^2) are (figures 13 and 14):

pavement	deflections (µm)							SCI (µm)	elastic moduli (N/mm ²)		bedding constant c (N/mm ³)	joint stiffness k (N/mm)	k/c
	d ₀	d ₂₀₀	d ₃₀₀	d ₅₀₀	d ₁₀₀₀	d ₁₅₀₀	d ₂₀₀₀		E ₀	E ₃			
ECT													
section I, M	521	419	-	229	131	90	69	292	103	265	0,12	24	200
section I, T	500	388	-	203	121	83	68	297	105	690	0,12	24	200
section VI	371	216	-	141	72	44	33	230	217	2085	0,12	24	200
section VII	330	234	-	155	103	70	55	175	130	2550	0,17	34	200
measurement 63	482	315	-	145	73	46	33	337	217	2020	0,09	18	200
TC													
site	759	546	396	255	123	-	62	504	115	310	0,06	12	200
exit, M	452	342	208	140	88	-	31	312	231	620	0,095	19	200
exit, T	609	413	297	209	118	-	59	400	121	325	0,09	17	190
Delft													
no. 2, T/M	681	-	363	185	108	76	55	496	130	-	0,085	11	130
no. 7, T/M	1315	-	601	341	190	125	97	974	73	-	0,04	6	150
no. 10A+B, T/M	894	-	415	234	125	86	67	660	106	-	0,06	8	135
no. 19, T	876	-	479	282	175	118	82	594	87	-	0,06	12	200
PP													
80 mm c.b.	1755	-	423	221	95	67	52	1534	137	-	0,028	3	107
120 mm c.b.	1676	-	432	251	95	63	49	1425	146	-	0,028	2,5	90

Table 3. Review of the pavements analyzed with ICES STRUDL: measured deflections and calculated elastic moduli of the sand subbase plus the subgrade (E₀) and the base (E₃), bedding constant (c) and joint stiffness (k).

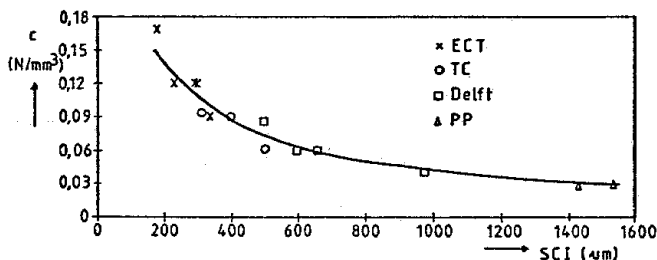


Figure 11. Mastercurve for the relationship between the bedding constant c and the surface curvature index SCI.

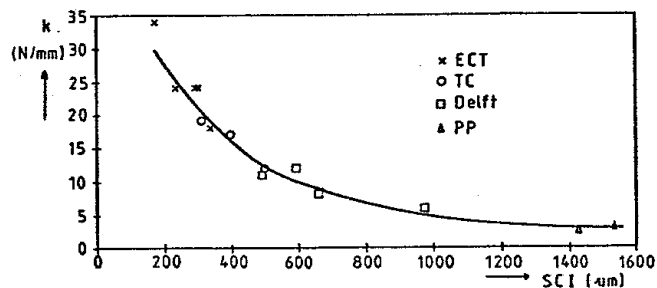


Figure 12. Mastercurve for the relationship between the joint stiffness k and the surface curvature index SCI.

$$c = 0,0444 + 0,000000019 \cdot E_{eq}^{2,9} \cdot e^{-0,0053 \cdot E_{eq}} \quad (16)$$

$$r = 0,76$$

$$k = 5,8523 + 0,000007668 \cdot E_{eq}^{2,8} \cdot e^{-0,0051 \cdot E_{eq}} \quad (17)$$

$$r = 0,81$$

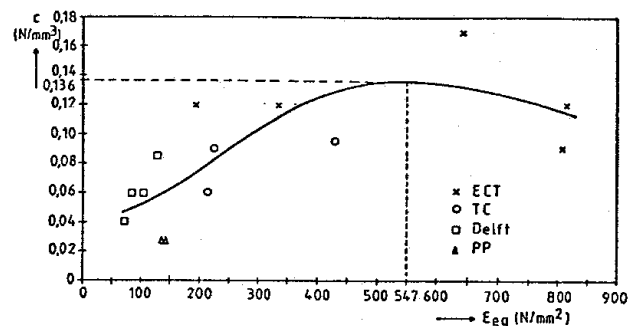


Figure 13. Mastercurve for the relationship between the bedding constant c and the equivalent elastic modulus of the substructure E_{eq}.

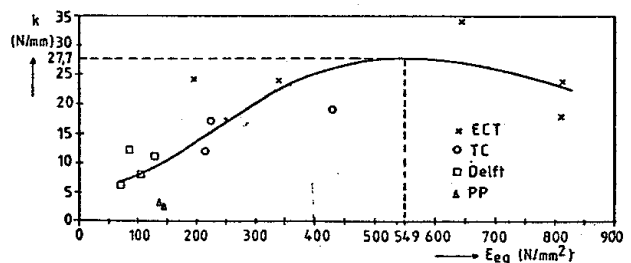


Figure 14. Mastercurve for the relationship between the joint stiffness k and the equivalent elastic modulus of the substructure E_{eq}.

The shape of these relations can be explained as follows:
In case of a low E_{eq}-value the directly loaded blocks are punched to a certain amount into the weak substructure, so the load transfer to

adjacent blocks is limited. In case of a very large E_{eq} -value under loading the total displacements, ϵ_{eq} and by that also the relative displacements of the blocks, are limited, so between the blocks hardly any shear forces can develop; for the main part the load is carried by the very stiff substructure.

The bedding constant c and the joint stiffness k have their maximum value at an equivalent elastic modulus of the substructure $E_{eq} \approx 550 \text{ N/mm}^2$. This means:

- strengthening of the substructure in case of $E_{eq} < 550 \text{ N/mm}^2$ (e.g. an unbound base on a sand subbase) yields an extra strengthening of the pavement due to an increasing load spreading in the concrete block layer and in the bedding sand layer
- strengthening of the substructure in case of $E_{eq} > 550 \text{ N/mm}^2$ is partly reduced due to a decreasing load spreading in the concrete block layer and in the bedding sand layer.

3.5 Relationship between the bedding constant c respectively the joint stiffness k , the equivalent elastic modulus of the substructure E_{eq} and the traffic loading n for the Delft pavements

By means of the equations 2, 13 and 14 relations between the bedding constant c (N/mm^3) respectively the joint stiffness k (N/mm) and the traffic loading n can be determined for the Delft pavements. These relations are (figures 15 and 16):

$$c = \frac{x - y \log n}{(38,08488 + 0,147263 \cdot (x - 200 - y \log n))^2} \quad (18)$$

$$k = \frac{x - y \log n}{(1,932189 + 0,005022 \cdot (x - 200 - y \log n))^3} \quad (19)$$

where: class C, T: $x = 1985$ $y = 247$
 M: $x = 2017$ $y = 249$
 class E, T: $x = 1498$ $y = 171$
 M: $x = 1549$ $y = 183$

Figure 15 shows, like figure 6, that the load spreading in the concrete block layer increases with increasing traffic loading.

Finally the figures 17 and 18, that were composed from the equations 4, 18 and 19, show that for the inner wheeltrack of the Delft pavements both the equivalent elastic modulus of the substructure E_{eq} ($= E_0$) and the bedding constant c and the joint stiffness k increase with increasing traffic loading n .

4. COMPARISON OF LINEAR-ELASTIC MULTILAYER THEORY AND FINITE ELEMENT METHOD FOR THE DELFT PAVEMENTS

In this chapter for the Delft pavements a comparison is made between the two evaluation methods considered in this paper. The comparison is only done for the inner wheeltrack (T) and for a 50 kN falling weight load.

In behalf of the comparison complementary calculations were carried out both with the linear-elastic multilayer program CIRCLY and with the finite element program ICES STRUDL. Considering

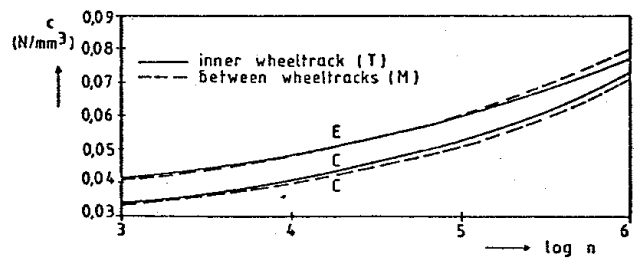


Figure 15. Relationship between the bedding constant c and the traffic loading n for the Delft pavements.

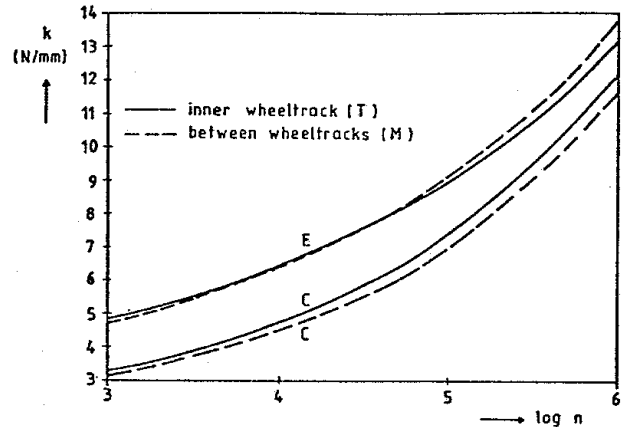


Figure 16. Relationship between the joint stiffness k and the traffic loading n for the Delft pavements.

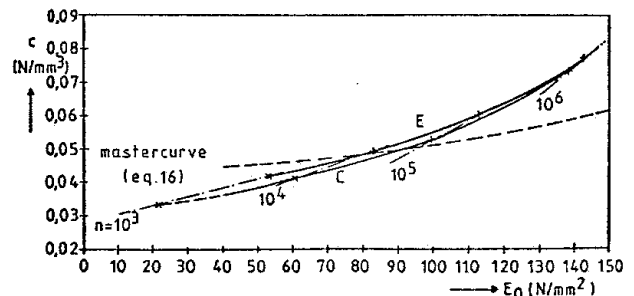


Figure 17. The effect of the traffic loading n on the bedding constant c and the equivalent elastic modulus of the substructure E_{eq} ($= E_0$) for the Delft pavements (inner wheeltrack).

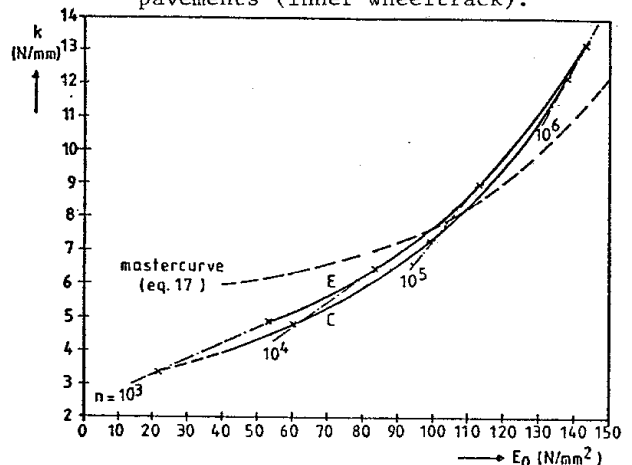


Figure 18. The effect of the traffic loading n on the joint stiffness k and the equivalent elastic modulus of the substructure E_{eq} ($= E_0$) for the Delft pavements (inner wheeltrack).

the Delft subgrade (clay, CBR-value 2 to 4%) the minimum elastic modulus of the substructure E_0 was set at $E_{0,min} = 40 \text{ N/mm}^2$; the calculations were made for E_0 -values ranging from 40 through 140 N/mm^2 (figure 5). In the CIRCLY calculations the elastic modulus of the concrete block layer E_1 , that goes with E_0 , is determined by means of equation 5a or 5c (figure 6). In the STRUDL calculations the bedding constant c and the joint stiffness k , that go with E_0 , are determined by means of equation 18 respectively 19 (figure 15 respectively 16). Table 4 shows the calculated combinations of E_0 and E_1 (CIRCLY) respectively E_0 , c and k (STRUDL) at the associated traffic loading n .

To illustrate the comparison some calculated deflection curves are shown in figure 19. From figure 19 one can observe that the very characteristic peaked deflection curve of concrete block pavements cannot be simulated well by means of the linear-elastic multilayer theory.

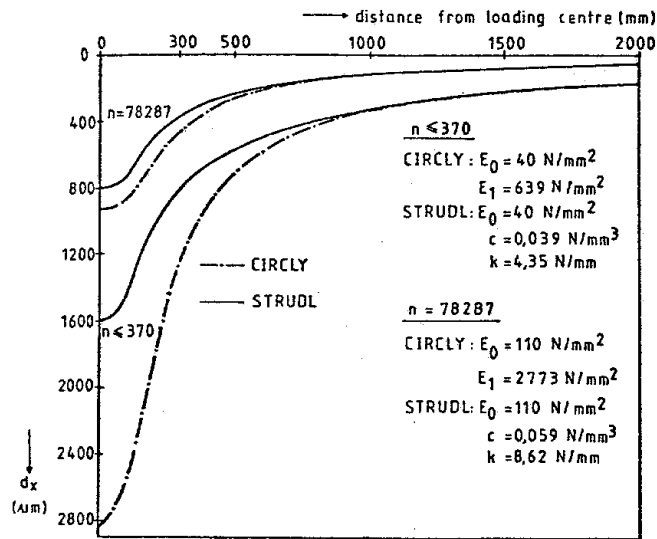


Figure 19. Some calculated deflection curves for the Delft pavements (class E).

On basis of the CIRCLY and STRUDL calculations a number of relations between the deflection d (μm) on a certain horizontal distance (mm) from the

load centre or on a certain depth z (mm) below the load centre and the traffic loading n were determined. These relations are:

class C, T

CIRCLY

$$\begin{aligned} \text{SCI} &= 373 + 49085.e^{-\log n} & r &= 1,00 \text{ (20a)} \\ d_0 &= 548 + 66403.e^{-\log n} & r &= 1,00 \text{ (20b)} \\ d_{z=80}-d_{z=1180} &= 435 + 53800.e^{-\log n} & r &= 1,00 \text{ (20c)} \\ d_{z=1180} &= 109 + 11477.e^{-\log n} & r &= 1,00 \text{ (20d)} \end{aligned}$$

STRUDL

$$\begin{aligned} \text{SCI} &= 442 + 23212.e^{-\log n} & r &= 0,97 \text{ (21a)} \\ d_0 &= 620 + 35937.e^{-\log n} & r &= 0,98 \text{ (21b)} \\ d_{z=80}-d_{z=1180} &= 527 + 26372.e^{-\log n} & r &= 0,97 \text{ (21c)} \\ d_{z=1180} &= 93 + 9565.e^{-\log n} & r &= 1,00 \text{ (21d)} \end{aligned}$$

class E, T

CIRCLY

$$\begin{aligned} \text{SCI} &= 492 + 20761.e^{-\log n} & r &= 1,00 \text{ (22a)} \\ d_0 &= 707 + 27477.e^{-\log n} & r &= 1,00 \text{ (22b)} \\ d_{z=80}-d_{z=1580} &= 609 + 23571.e^{-\log n} & r &= 1,00 \text{ (22c)} \\ d_{z=1580} &= 103 + 3420.e^{-\log n} & r &= 1,00 \text{ (22d)} \end{aligned}$$

STRUDL

$$\begin{aligned} \text{SCI} &= 491 + 7988.e^{-\log n} & r &= 0,95 \text{ (23a)} \\ d_0 &= 697 + 12909.e^{-\log n} & r &= 0,97 \text{ (23b)} \\ d_{z=80}-d_{z=1580} &= 602 + 9819.e^{-\log n} & r &= 0,96 \text{ (23c)} \\ d_{z=1580} &= 95 + 3090.e^{-\log n} & r &= 1,00 \text{ (23d)} \end{aligned}$$

The quotients f of the STRUDL calculated deflections and the CIRCLY calculated deflections are:

class C					class E				
n	E_0 (N/mm^2)	E_1 (N/mm^2)	c (N/mm^3)	k (N/mm)	n	E_0 (N/mm^2)	E_1 (N/mm^2)	c (N/mm^3)	k (N/mm)
≤ 2945	40	783	0,037	3,94	≤ 370	40	639	0,039	4,35
5331	50	1103	0,039	4,31	795	50	944	0,041	4,73
9650	60	1424	0,041	4,74	1708	60	1248	0,043	5,17
17469	70	1744	0,044	5,24	3671	70	1553	0,046	5,68
31623	80	2065	0,046	5,82	7889	80	1858	0,048	6,25
57244	90	2385	0,050	6,50	16953	90	2163	0,051	6,92
103625	100	2705	0,053	7,30	36430	100	2468	0,055	7,71
187584	110	3026	0,057	8,26	78287	110	2773	0,059	8,62
339569	120	3346	0,062	9,42	168234	120	3078	0,063	9,71
614695	130	3666	0,068	10,82	361526	130	3383	0,069	11,01
1112735	140	3987	0,075	12,55	776901	140	3688	0,075	12,57

Table 4. Combinations of elastic moduli E_0 and E_1 , bedding constant c and joint stiffness k for the Delft pavements in behalf of CIRCLY and STRUDL calculations.

class C, T

$$\text{SCI: } f = 0,892 - 0,111 \cdot (\log n - 5,2)^2$$

$$r = -1,00 \quad (24a)$$

$$d_0: f = 0,902 - 0,094 \cdot (\log n - 5,2)^2$$

$$r = -1,00 \quad (24b)$$

$$d_{z=80}-d_{z=1180}: f = 0,929 - 0,114 \cdot (\log n - 5,2)^2$$

$$r = -1,00 \quad (24c)$$

$$d_{z=1180}: f = 0,849 - 0,011 \cdot (\log n - 4,65)^2$$

$$r = -0,96 \quad (24d)$$

class E, T

$$\text{SCI: } f = 0,839 - 0,058 \cdot (\log n - 5,0)^2$$

$$r = -1,00 \quad (25a)$$

$$d_0: f = 0,864 - 0,050 \cdot (\log n - 5,0)^2$$

$$r = -1,00 \quad (25b)$$

$$d_{z=80}-d_{z=1580}: f = 0,855 - 0,056 \cdot (\log n - 5,0)^2$$

$$r = -1,00 \quad (25c)$$

$$d_{z=1580}: f = 0,926 - 0,008 \cdot (\log n - 4,15)^2$$

$$r = -0,99 \quad (25d)$$

From the equations 20 through 25 one can observe that in case of $n < 10^6$ the CIRCLY calculated deflections are always larger than the STRUDL calculated deflections. The biggest differences occur at points on a horizontal and/or vertical distance of less than 1 m from the load centre at a limited number of load repetitions n (see also figure 19).

In chapter 3 it is shown that there is an excellent correspondence between measured and STRUDL calculated deflection curves. However, the correction factors f (equations 24 and 25) enable to use linear-elastic multilayer calculations in a justified manner. These linear-elastic multilayer models are, in contrast with finite element programs like ICES STRUDL, rather cheap in use and general available by tables and graphs (Burmister, Jones etc.) and computer programs like CIRCLY (6) and BISAR (12).

5. CALCULATION OF RUTTING ON THE DELFT PAVEMENTS

Rutting is the most important defect that can be observed on concrete block pavements. On basis of rut depth measurements on the Delft pavements no rutting models could be developed, because on most pavements the concrete blocks were relaid in the past (4). Therefore the progress of rutting on the Delft pavements will be calculated by means of permanent deformation models.

5.1 Permanent deformation models for concrete block pavements

The rut depth calculations will be based on the permanent deformation models developed by the Belgian Road Research Laboratory for use in the design of flexible pavements (13,14). However,

concrete block pavements show an increasing load spreading with increasing number of load repetitions n , and for this reason the permanent deformation models have to be modified in the following sense (figure 20):

$$\frac{d(\Delta h_p)}{dn} = f_1 \cdot \frac{df_2}{dn} \quad (26)$$

where: Δh_p = permanent deformation in a layer of unbound material

f_1 = elastic compression of the layer due to a standard axle load

f_2 = permanent deformation relation

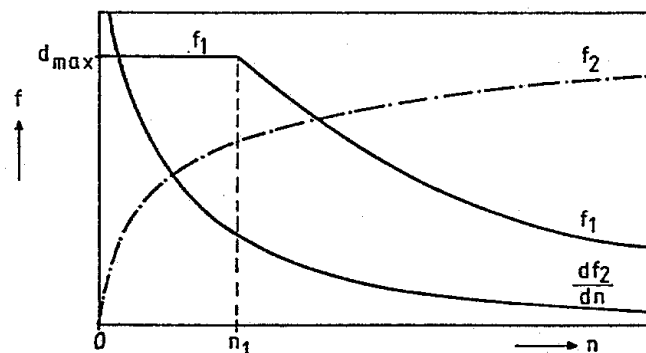


Figure 20. Schematic representation of permanent deformation functions.

The relation f_2 is (13,14):

$$\text{granular material: } f_2 = a \cdot n^b \quad (27a)$$

$$\text{cohesive material: } f_2 = a + b \cdot \log n \quad (27b)$$

For concrete block pavements was found (figure 20) a minimum E_0 -value, so maximum deflections d_{max} , in case of $n \leq n_1$ and an increasing E_0 -value, so decreasing deflections (equations 21 and 23), in case of $n > n_1$. Therefore the function f_1 is:

$$n \leq n_1: f_1 = d_{max} = \text{constant} \quad (28a)$$

$$n > n_1: f_1 = p + q \cdot e^{-\log n} \quad (28b)$$

The permanent deformation in a layer of unbound material in a concrete block pavement is obtained by combining the equations 26, 27 and 28:

granular material

$$n \leq n_1: \Delta h_p = \int_0^n d_{max} \cdot a \cdot b \cdot n^{b-1} \cdot dn = d_{max} \cdot a \cdot n^b \quad (29a)$$

$$n > n_1: \Delta h_p = \int_0^{n_1} d_{max} \cdot a \cdot b \cdot n^{b-1} \cdot dn +$$

$$+ \int_{n_1}^n (p + q \cdot e^{-\log n}) \cdot a \cdot b \cdot n^{b-1} \cdot dn =$$

$$= d_{max} \cdot a \cdot n_1^b + a \cdot p \cdot (n^b - n_1^b) +$$

$$+ \frac{a \cdot b \cdot q}{b - 0,4343} \cdot (n^{b-0,4343} - n_1^{b-0,4343}) \quad (29b)$$

cohesive material

$$n \leq n_1: \Delta h_p = \int_0^{n_1} d_{\max} \cdot \frac{b}{\ln 10} \cdot \frac{1}{n} \cdot dn = d_{\max} \cdot (a + b \log n) \quad (30a)$$

$$n > n_1: \Delta h_p = \int_0^{n_1} d_{\max} \cdot \frac{b}{\ln 10} \cdot \frac{1}{n} \cdot dn + \int_{n_1}^n (p + q \cdot e^{-\log n}) \cdot \frac{b}{\ln 10} \cdot \frac{1}{n} \cdot dn =$$

$$= d_{\max} \cdot (a + b \log n_1) + b \cdot p \cdot \log \frac{n}{n_1} - b \cdot q \cdot (n^{-0,4343} - n_1^{-0,4343}) \quad (30b)$$

5.2 Rut depth calculations for the Delft pavements

In the calculation of the progress of rutting on the Delft pavements by means of the equations 29 and 30 three assumptions were made:

1. permanent deformation coefficients (13,14):
sand subbase: $a = 2$ $b = 0,3$
clay subgrade: $a = 1$ $b = 0,7$
2. channellized traffic
3. the 80 kN standard axle loads have single wheels, load 40 kN (= 0,8 times the falling weight load) and diameter contact area 300 mm (= diameter falling weight loading plate), so the contact pressure is $0,8 \times 0,707 = 0,566$ N/mm²; this assumption means that the deflections according to the equations 21 and 23 have to be multiplied by 0,8.

With these assumptions for the Delft pavements the permanent deformation in the sand subbase ($\Delta h_{p,sa}$) and in the clay subgrade ($\Delta h_{p,su}$) were calculated by means of equation 29 respectively 30 (tables 5 and 6). The permanent deformation in the subgrade is very small compared with the permanent deformation in the sand subbase.

The rut depth RD is:

$$RD = \Delta h_{p,sa} + \Delta h_{p,su} \quad (31)$$

The progress of the rut depth as a function of the traffic loading n is shown in figure 21. By means of linear regression analysis for the rut depth RD (mm) equations alike

$$RD = a \cdot n^b \quad (32)$$

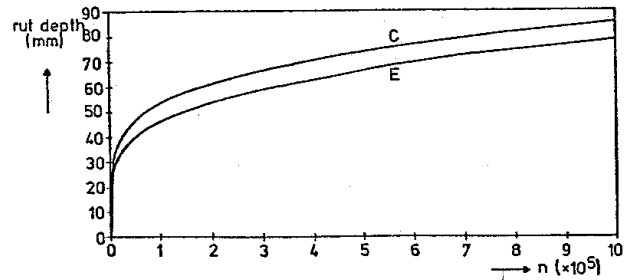


Figure 21. Calculated rut depth on the Delft pavements as a function of the number of equivalent 80 kN standard axle loads (single wheels).

sand subbase ($h_{sa} = 1,1$ m)		clay subgrade												
$a = 2$		$a = 1$												
$b = 0,3$		$b = 0,7$												
$d_{\max} = 0,8 \cdot (d_{z=80} - d_{z=1180})_{\max} = 1015 \mu\text{m}$		$d_{\max} = 0,8 \cdot (d_{z=1180})_{\max} = 316 \mu\text{m}$												
$p = 0,8 \cdot 527 = 422 \mu\text{m}$		$p = 0,8 \cdot 93 = 74 \mu\text{m}$												
$q = 0,8 \cdot 26372 = 21098 \mu\text{m}$		$q = 0,8 \cdot 9565 = 7652 \mu\text{m}$												
$n_1 = 2945$		$n_1 = 2945$												
Δh_p (mm) \ n	100	200	500	1000	2000	5000	10000	20000	50000	100000	200000	500000	1000000	
$\Delta h_{p,sa}$	8,08	9,95	13,10	16,12	19,85	26,10	31,28	36,81	44,90	51,87	59,83	72,34	83,78	
$\Delta h_{p,su}$	0,76	0,82	0,91	0,98	1,05	1,13	1,18	1,22	1,27	1,29	1,32	1,35	1,37	
RD (mm)	8,84	10,77	14,01	17,10	20,90	27,23	32,46	38,03	46,17	53,16	61,15	73,69	85,15	

Table 5. Rut depth calculation for the Delft pavements, class C (sand subbase thickness 1,1 m).

sand subbase ($h_{sa} = 1,5$ m)		clay subgrade												
$a = 2$		$a = 1$												
$b = 0,3$		$b = 0,7$												
$d_{\max} = 0,8 \cdot (d_{z=80} - d_{z=1580})_{\max} = 1012 \mu\text{m}$		$d_{\max} = 0,8 \cdot (d_{z=1580})_{\max} = 262 \mu\text{m}$												
$p = 0,8 \cdot 602 = 482 \mu\text{m}$		$p = 0,8 \cdot 95 = 76 \mu\text{m}$												
$q = 0,8 \cdot 9819 = 7855 \mu\text{m}$		$q = 0,8 \cdot 3090 = 2472 \mu\text{m}$												
$n_1 = 370$		$n_1 = 370$												
Δh_p (mm) \ n	100	200	500	1000	2000	5000	10000	20000	50000	100000	200000	500000	1000000	
$\Delta h_{p,sa}$	8,06	9,92	13,10	15,89	18,89	23,34	27,20	31,64	38,66	45,12	52,83	65,49	77,44	
$\Delta h_{p,su}$	0,63	0,68	0,76	0,80	0,84	0,88	0,91	0,93	0,96	0,98	1,00	1,03	1,04	
RD (mm)	8,69	10,60	13,86	16,69	19,73	24,22	28,11	32,57	39,62	46,10	53,83	66,52	78,48	

Table 6. Rut depth calculation for the Delft pavements, class E (sand subbase thickness 1,5 m).

were determined. The result of this analysis was:

$$\text{class C: } RD = 3,10.n^{0,246} \quad (32a)$$

$$\text{class E: } RD = 3,21.n^{0,233} \quad (32b)$$

6. DESIGN CHARTS FOR CONCRETE BLOCK PAVEMENTS WITH A SAND SUBBASE

In a similar way as described in section 5.2 a number of rut depth calculations was carried out for an initial E_0 -value ranging from 40 through 140 N/mm^2 . At $E_0 = 40 \text{ N/mm}^2$ the subgrade was supposed to be a cohesive material (tables 5 and 6), at $E_0 = 140 \text{ N/mm}^2$ the subgrade was supposed to be a granular material (sand); at intermediate E_0 -values a gradual interpolation between a cohesive and a granular material was applied.

On basis of these rut depth calculations design charts for concrete block pavements, consisting of 80 mm thick rectangular concrete blocks in herringbone bond and a sand subbase, were developed (figure 22); these design charts cover most Dutch subgrade conditions. With the design charts the pavement life, in case of an acceptable rut depth of 15, 25 or 35 mm, can be determined as a function of the initial elastic modulus of the substructure E_0 , the thickness of the sand subbase and the number of equivalent 80 kN standard axle loads per lane per day.

From the analysis of the Delft pavements only design curves for sand subbase thicknesses of 1,5 and 1,1 m could be derived. Based on a limited number of STRUDL calculations tentative design curves for a sand subbase thickness of 0,7 m are presented too.

7. CONCLUSIONS

Based on the results of the analysis of a number of concrete block pavements as presented here, the following main conclusions can be drawn:

1. Falling weight deflection measurements carried out in the city of Delft on 17 in service concrete block pavements, consisting of 80 mm thick rectangular concrete blocks in herringbone bond and a sand subbase, showed a decrease of all deflections as well as the surface curvature index with increasing number of load repetitions.
2. By means of the finite element method, in which the concrete blocks are represented as indeformable rigid bodies, an excellent correspondence between calculated and measured deflection curves is obtained. The deflection curves calculated by means of the linear-elastic multilayer theory are different from the measured deflection curves, especially in case of a limited number of load repetitions.
3. The elastic modulus of the substructure (sand subbase plus subgrade), the bedding constant and the joint stiffness all increase with increasing traffic loading, resulting in a substantial progressive stiffening of the total concrete block pavement.
4. It has been possible to incorporate this progressive stiffening in rut depth calculations, therefore it is believed that for Dutch conditions realistic design charts were developed

for concrete block pavements, consisting of 80 mm thick rectangular concrete blocks in herringbone bond and a sand subbase.

5. Good relations exist between the bedding constant respectively the joint stiffness on one hand and the surface curvature index on the other hand; these relations also cover concrete block pavements having a bound or unbound base.
6. Both the bedding constant and the joint stiffness reach their maximum value at an equivalent elastic modulus of the substructure (base plus sand subbase plus subgrade) of 550 N/mm^2 .

8. ACKNOWLEDGEMENTS

The research reported was sponsored by the Department of Civil Engineering of the Delft University of Technology.

Special acknowledgements are made to mr. A.C. Pruyssers, J. Elzenaar and H.F.L. Jansen for carrying out all the measurements.

9. REFERENCES

- (1) Houben, L.J.M.
Concrete Block Paving
Proceedings FURORIS Congress, University of Suriname/Delft University of Technology, 1982
- (2) Pelt, A.M.A.M. van, Houben, L.J.M. and Molenaar, A.A.A.
Research into the Structural Behaviour of two prototype Concrete Block Pavements, subjected to Repeated Plate Loadings (in Dutch)
Report 7-82-200-2, Laboratory for Road and Railroad Research, Delft University of Technology, 1982
- (3) Pelt, A.M.A.M. van, Houben, L.J.M. and Molenaar, A.A.A.
Research into the Structural Behaviour of two prototype Concrete Block Pavements, subjected to Repeated Plate Loadings (in Dutch)
Wegen, Vol. 57, no. 2, 1983
- (4) Fuchs, G.H.A.M., Houben, L.J.M. and Molenaar, A.A.A.
Analysis of in service Concrete Block Pavements (in Dutch)
Report 7-83-200-5, Laboratory for Road and Railroad Research, Delft University of Technology, 1983
- (5) Molenaar, A.A.A. and Velden, G. van der
Tables for the Calculation of Elastic Moduli from Deflection Measurements (in Dutch)
Report 7-77-5-115-2, Laboratory for Road and Railroad Research, Delft University of Technology, 1977
- (6) Wardle, L.J.
Program CIRCLY - A Computer Program for the Analysis of Multiple Complex Circular Loads on Layered Anisotropic Media
Division of Applied Geomechanics, Commonwealth Scientific and Industrial Research Organisation, Australia, 1977

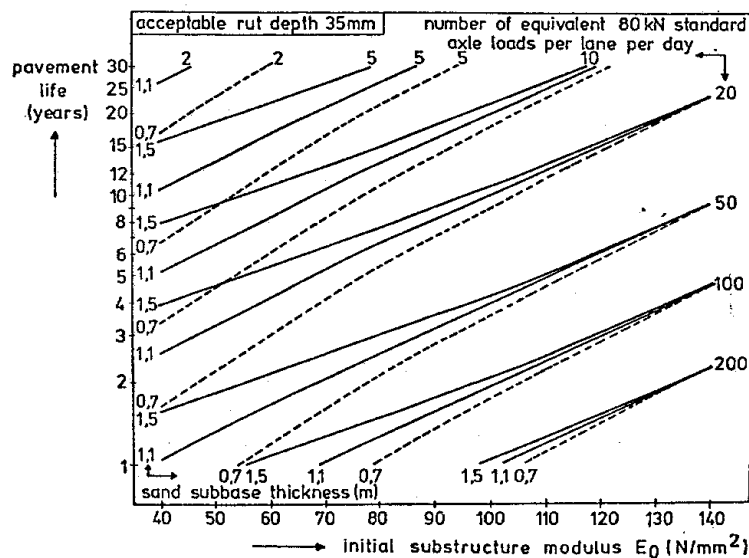
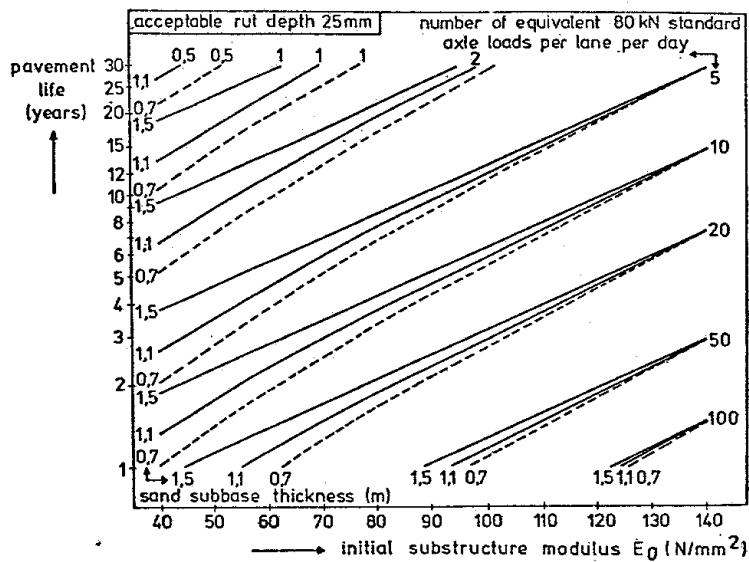
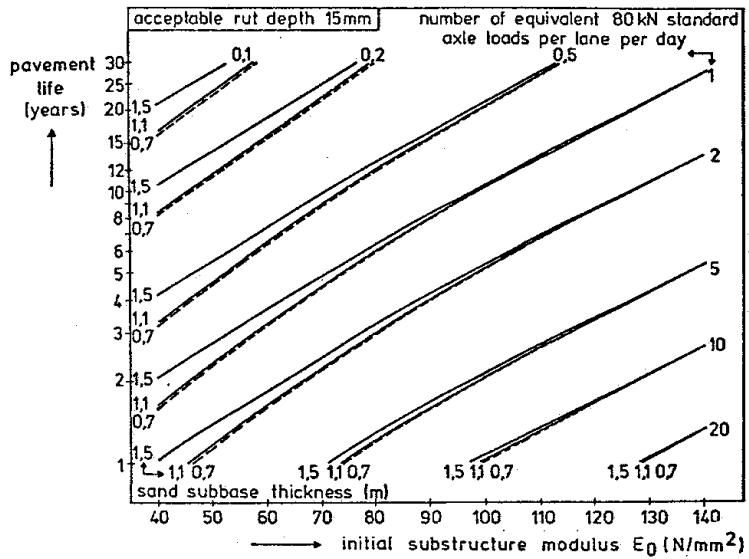


Figure 22. Design charts for concrete block pavements, consisting of 80 mm thick rectangular concrete blocks in herringbone bond and a sand subbase.

- (7) Kok, A.W.M.
ICES STRUDL, RIGID BODIES
Structural Mechanics Division, Department
of Civil Engineering, Delft University of
Technology, 1982
- (8) Moll, H.O. and Molenaar, A.A.A.
*Application of the Finite Element Method on
Concrete Block Pavements (in Dutch)*
Memorandum 7-83-200-6-M, Laboratory for
Road and Railroad Research, Delft Universi-
ty of Technology, 1983
- (9) Moll, H.O., Vroom, J.A. and Molenaar, A.A.A.
*Method for the Evaluation of the Concrete
Block Pavement of the Europe Container Ter-
minus Home Terminal (in Dutch)*
Memorandum 7-82-200-5-M, Laboratory for
Road and Railroad Research, Delft Universi-
ty of Technology, 1982
- (10) Claessen, A.I.M., Edwards, J.M., Sommer, P.
and Ugé, P.
Asphalt Pavement Design - The Shell Method
Proceedings Fourth International Conference
Structural Design of Asphalt Pavements, Ann
Arbor, 1977
- (11) Ivanov, N.N.
*Calculation of Flexible Pavements, subjected
to Repeated Dynamic Loads (in French)*
Revue Générale des Routes et des Aérodrômes,
no. 294, 1962
- (12) Jong, D. de, Peutz, M. and Korswagen, A.
*Computer Program BISAR - Layered Systems un-
der Normal and Tangential Surface Loads*
External Report AMSR.0006.73, Koninklijke/
Shell Laboratorium, Amsterdam, 1973
- (13) Veverka, V.
*Evaluation of the Rut Depth in Flexible Pa-
vements (in Dutch)*
De Wegentechniek, Vol. 24, no. 3, 1979
- (14) Verstraeten, J., Veverka, V. and Francken, L.
*Rational and Practical Designs of Asphalt
Pavements to avoid Cracking and Rutting*
Proceedings Fifth International Conference
Structural Design of Asphalt Pavements,
Delft, 1982